

SN and BAO constraints on (new) polynomial dark energy parametrizations: current results and forecasts

Irene Sendra^{1*} and Ruth Lazkoz^{1†}

¹*Fisika Teorikoa, Zientzia eta Teknologia Fakultatea, Euskal Herriko Unibertsitatea UPV/EHU, 644 Posta Kutxatila, 48080 Bilbao, Spain*

October 3, 2018

ABSTRACT

In this work we introduce two new polynomial parametrizations of dark energy and explore their correlation properties. The parameters to fit are the equation of state values at $z = 0$ and $z = 0.5$, which have naturally low correlation and have already been shown to improve the popular Chevallier-Polarski-Linder (CPL) parametrization. We test our models with low redshift astronomical probes: type Ia supernovae and baryon acoustic oscillations (BAO), in the form of both current and synthetic data. Specifically, we present simulations of measurements of the radial and transversal BAO scales similar to those expected in a BAO high precision spectroscopic redshift survey similar to EUCLID. According to the Bayesian deviance information criterion (DIC), which penalizes large errors and correlations, we show that our models perform better than the CPL re-parametrization proposed by Wang (in terms of $z = 0$ and $z = 0.5$). This is due to the combination of a lower correlation and smaller relative errors. The same holds for a frequentist perspective: our Figure-of-Merit is larger for our parametrizations.

Key words: cosmology: dark energy, observations, cosmological parameters

1 INTRODUCTION

More than a decade ago it was discovered that the universe is expanding with increasing velocity, and this fact was brought to light by type Ia Supernovae (SN) observations (Perlmutter et al. 1999; Riess et al. 1998, 2004; Astier et al. 2006). Nowadays the accelerated expansion of the universe stands as confirmed by several independent observations as the already mentioned SNeIa (Hawkins et al. 2003; Goldstein et al. 2003; Readhead et al. 2004; Tegmark et al. 2004; Spergel et al. 2007); the measurements of cluster properties as the mass, the correlation function and the evolution with redshift of their abundance (Eke et al. 1998; Viana et al. 2002; Bahcall et al. 2003; Bahcall & Bode 2003); the optical surveys of large scale structure (Pope et al. 2004; Cole et al. 2005; Eisenstein et al. 2005); the anisotropies in the Cosmic Microwave Background (CMB) (de Bernardis et al. 2000; Spergel et al. 2003; Komatsu et al. 2011); the cosmic shear measured from weak lensing (Van Waerbeke et al. 2001; Refregier 2003) and the Lyman- α forest absorption (Croft et al. 1999; McDonald et al. 2005).

This accelerated expansion can be explained postulating the existence of a “new” component in the universe,

called “dark energy” which would represent about between the 70% – 75% the of the mass-energy of the universe and would counteract the effects of the gravitational attraction. The remaining 25 – 20% would be composed by dark matter mainly and about an extra 5% which would account for the baryons, radiation and neutrinos. Although the existence of the dark energy is well established observationally, there is not a entirely compelling theoretical model which gives a theoretical physical framework within which the dark energy can be understood, and is of course compliant with all main observations.

Observational data agree rather well with the simplest model, Λ CDM, which puts down the acceleration to the presence of a cosmological constant Λ . This model has become the standard model of cosmology due to its simplicity and compliance with the data, but there are still some points that it can not account, e.g. the small value of the cosmological constant, which cannot be explained in terms of any of the known interactions.

This situation leads to the proposal of other settings which admit a slightly time-variable dark energy as the agent producing the the cosmic acceleration. Many such models have emerged along theoretical avenues: quintessence (Zlatev et al. 1999), Chaplygin gas (Bento et al. 2002), modified gravity (Nojiri & Odintsov 2006), holographic dark energy (Li 2004), braneworld models (Maartens 2005), $f(R)$

* E-mail: irene.sendra@ehu.es

† E-mail: ruth.lazkoz@ehu.es

theories (Sotiriou & Faraoni 2010), theories with extra dimensions (Lechtenfeld et al. 2002), and quite a few others. Unfortunately none of them have emerged as definitive answers for the dark energy problem, so currently the situation is one of quick advances on the empirical front (regarding the quantity and quality of the data), whereas theory is somewhat mired in a jungle of alternatives. Since it is not fully clear what the observations should be compared with, a try and tested approach, borrowed from many areas of physics, is defining a parametrization of dark energy functions which, if well designed, allows to encapsulate all the observational information in a few numbers which can afterwards be compared with theoretical predictions.

The most natural approach in this case is considering the dark energy equation of state. It is usually assumed that this quantity varies slowly with redshift and can be approximated by a fitting formula with a small number of free parameters. These parameters can be constrained comparing the ansatz with observations using an optimization procedure. Choices are typically built upon intuition and prior information, but there is yet plenty of room for discussion and improvements. This is precisely the direction we follow in this work.

In section 2 we propose two new polynomial parametrizations of dark energy. We perform cosmological tests to compare them to the most popular dark energy parametrization in the literature, both in its classical fashion and a new, improved reformulation. We resort to several criteria to perform our comparison: in addition to the χ^2 value, we also pay attention to the correlation of the coefficients, figure of merit, fractional errors on the free dark energy parameters and the deviance information criterion (DIC). The reason for an analysis from several perspectives is that we find χ^2 to be an insufficiently informative tool, as it does not offer any reward upon some important improvements like tighter constraints or lower correlation.

Our tests make use of Type Ia supernovae (SN) and baryon acoustic oscillations (BAO), which are so far the best representatives in the categories of standard candles (objects with well determined intrinsic luminosity) and standard rulers (objects with well determined comoving size). Such probes provide us with distance measures related to the Hubble factor $H(z)$, and as they are low redshift datasets, their suitability to constrain dark energy is strong, as this component of the cosmic soup has begun to govern the evolution of the Universe just recently, according to most evidences. This combination has additional advantages: SN measurements come in the form of luminosity distances and therefore give a smeared out information on $H(z)$ (two integrations are required) but still remain extremely useful because of the large number of measurements and their considerably good quality. On the other hand, BAO measurements, though currently scarce, involve $1/H(z)$ directly, so they are expected to favour sensitivity considerably, besides being of even better quality than SN data. In principle, one could also consider including CMB data, but typically they do not improve constraints on dark energy parameters significantly (WMAP7-year data alone constrain w in quiescence models with about a 40% error), and the dark matter density Ω_m is generally the only parameter on which those data exert a strong impact. A good compromise between simplic-

ity and advantages offered by CMB as regards Ω_m is the use of priors, and that is the approach we use.

Interestingly, we will not only use the latest observational data to obtain the constraints on the parameters of the models, but we will also consider mock data simulating a forthcoming survey, as described in sections 3. We present the mock datasets for the two main measurable quantities expected from a line-of-sight, high-resolution spectroscopic baryon acoustic oscillations survey (Percival 2010; EUCLID EUCLID; Refregier et al. 2010; Beaulieu et al. 2010), as it has been done in a previous work (Escamilla-Rivera et al. 2011).

We combine these data with synthetic pre-WFIRST (Wide-Field Infrared Survey Telescope) supernovae data to throw further light on the constraining power and suitability of the parametrizations proposed, so we are allowed to strengthen our conclusions.

2 DARK ENERGY PARAMETRIZATIONS

The Friedman equations explain how an homogeneous and isotropic universe expands in the context of General Relativity (or generalizations). Considering such a universe is filled with several fluid components with pressures p_i and energy densities ρ_i , those equations will read

$$H^2 \equiv \left(\frac{\dot{a}}{a}\right)^2 = \frac{8\pi G}{3} \sum_i \rho_i - \frac{k}{a^2} \quad (1)$$

$$\frac{\ddot{a}}{a} = -\frac{4\pi G}{3} \sum_i (\rho_i + 3p_i), \quad (2)$$

where a and H are the scale and Hubble factor respectively. At present, the two main such fluids are dark matter and dark energy, the last being the governor. Dark energy (de) enters our picture in an effective way in the sense we do not appeal to any fundamental theory to deduce its behaviour and just let it be represented by a phenomenological equation of state (EOS):

$$w(z) = \frac{\rho_{de}}{p_{de}}. \quad (3)$$

The importance of the EOS is significant, because it determines the form of the Hubble parameter $H(z)$ or any derivation of it which is necessary to obtain the observable quantities. Under the spatial flatness assumption ($k=0$)

$$\frac{H^2(z)}{H_0^2} = \Omega_m(1+z)^3 + \Omega_{de}X(z) \quad (4)$$

with

$$X(z) = \frac{\rho_{de}(z)}{\rho_{de}(0)} = \exp\left(3 \int_0^z \frac{1+w(z)}{1+z} dz\right), \quad (5)$$

and $\Omega_{de} = 1 - \Omega_m$.

Considering the huge number of contributions to the topic, and the knowledge so far gathered it might seem hard to make improvements, but we believe some avenues opened by Wang in (Wang 2008) are worth exploring and allow for little but valuable advances towards parametrizations that make the best out of the data available. Questions like the most convenient choice of the two dark energy parameters or the most suitable model comparison criterion are worth being looked at once and again, particularly to build a more

solid background to make the most out of future data and their expected far better statistical value.

2.1 Chevallier-Polarski-Linder parametrization

The Chevallier-Polarski-Linder (CPL) parametrization, first discussed in (Chevallier & Polarski 2001) and reintroduced in (Linder 2003), defines the dark energy equation of state as

$$w(z) = w_0 + w_a \frac{z}{1+z}, \quad (6)$$

where w_0 is the value of the dark energy equation of state today (i.e. at redshift $z = 0$). This parametrization has been widely used because of its simplicity, sensitivity to observational data and because it is well behaved and bounded at high redshifts. Its adoption by the Dark Energy Task Force (Albrecht et al. 2009) as a preferred parametrization has contributed to its popularity.

However, this parametrization has shortcomings: its flexibility to determine cosmological parameters for some dark energy models with rapid evolution has been put in doubt recently, and on the other hand the second parameter is typically very poorly constrained thus losing power of conviction about the conclusions to be drawn from it.

2.2 Wang parametrization

The quest to delineate the expansion history of Universe is expected to make big ambitious moves in the future. As a result it is expected that many more and better observational data will be available. Obviously it is worth getting prepared to making the best profit out of this avalanche of data to come, and this can be done by learning as much as possible from the data we already. Intuitively, in order to be able to discern which dark energy model is closest to reality and to offer a sensible interpretation of the results it seems necessary to consider dark energy parameters which offer clear advantages. Apart from having a clear physical meaning, for a parameter to be eligible there should be previous hints or theoretical grounds forecasting reasonably tight constraints, and as it is well known, the parameter should be the least possibly correlated to others. Suitability criteria for parameters along those grounds can be sketched with the help of comparison tools rewarding for those nice features. The (frequentist) FoM favours low correlation whereas the (Bayesian) does not only favour that feature, but it also rewards for tight constraints also, so both these criteria (FoM and DIC) do poorly when high correlation is present in the dark energy parametrization one considers. In this respect, one must make a fair use of those statistical tools. For instance, if one takes performs a reparametrization of a certain scenario, the FoM and DIC as calculated for both cases will typically be direct indicators of improvements (or worsenings) in terms of correlation, but changes in the value of those quantities should not be held in the same grounds as the changes occurring when constraining the same single parametrization with two different datasets.

The CPL parametrization suffers from quite a significant correlation, besides the fact that constraints on one of its parameters are typically large in percentual terms. But on the other hand it has some nice features, so a convenient

redefinition as concerns those two issues was put forward to yield an improved situation, although the encoded information remains exactly the same. As mentioned, this was done in (Wang 2008), where a new dark energy description was given in terms of its value at present, w_0 , and at redshift $z = 0.5$, $w_{0.5}$, was given. Explicitly

$$w(z) = 3w_{0.5} - 2w_0 + \frac{3(w_0 - w_{0.5})}{1+z}, \quad (7)$$

was proposed, and this can be seen just as a rearrangement of the classic CPL parametrization. This reformulation minorates the correlation between the parameters and allows to obtain tighter constraints along with a more transparent interpretation of the parameter estimation results, just in the spirit of making an optimal use of observational data from future surveys.

The results in our paper reinforce the view that Eq. 7 is a preferred way of exploiting the CPL parametrization, and on the other hand we suggest, with the help of two new parametrizations, that the $(w_0, w_{0.5})$ couple is indeed a very good choice despite the specifics of the dark energy evolution, provided it is smooth enough and with bounded early asymptotic behaviour.

2.3 Polynomial parametrizations

The two proposals we are making are somewhat inspired on the one hand by the CPL parametrization and on the other hand by an a proposal consisting in a expansion in powers of the quantity $(1+z)$ which emerged naturally from the relationship between the redshift and the scale factor and showed computationally convenience. This second inspiring setup we are referring to was proposed for the first time in (Weller & Albrecht 2002) in the form

$$w(z) = -1 + c_1(1+z) + c_2(1+z)^2. \quad (8)$$

However, this sort of parametrization poses problems at high redshifts, as $|w(z)|$ grows unboundedly with z and one will either end up with a superphantom model or a superluminal one. This motivates considering generalizations which are devoid of this pathology and may match or even surpass the nicety of CPL or its reformulation (recall Eq. 7).

Two possible routes that retain some similarity with the previous case but also some improvements arise from

$$w(z) = -1 + c_1(1+f(z)) + c_2(1+f(z))^2. \quad (9)$$

with $f(z)$ a smooth and at the same time simple function or the slightly more general

$$w(z) = -1 + c_1 g_1(1+f(z)) + c_2 g_2(1+f(z)), \quad (10)$$

where g_1 and g_2 are some smooth and simple functions as well.

2.3.1 Conventional polynomial

In the spirit of the first scheme above we propose

$$f(z) = \frac{z}{1+z} \quad (11)$$

so we avoid high-redshift unboundedness by the same via as in CPL. Therefore we have

$$w(z) = -1 + c_1 \left(1 + \frac{z}{1+z}\right) + c_2 \left(1 + \frac{z}{1+z}\right)^2, \quad (12)$$

which we dub conventional polynomial parametrization. If more compactness is desired one can also write the latter as

$$w(z) = -1 + c_1 \left(\frac{1+2z}{1+z}\right) + c_2 \left(\frac{1+2z}{1+z}\right)^2. \quad (13)$$

It is convenient to leave out the constant term of value -1 from the computational point of view because as one does not expect a large departure from a Λ CDM setting, it is reasonable to confine (at least initially) the parameter search region to $|c_1| < 1$ and to $|c_2| < 1$.

However, as we have discussed already it is desirable to fit parameters which are more or less physically transparent and it in addition are just lightly correlated. At a first stage we wish to compare our conventional polynomial parametrization with Wang's, so the best way to do so is to consider exactly the same two dark energy parameters. Then, at a later stage, we will check whether the good behaviour as correlation is concerned is shared by our parametrization. With those arguments in mind we reformulate the proposal made in Eq. 13 by letting

$$c_1 = \frac{1}{4}(16w_0 - 9w_{0.5} + 7), \quad (14)$$

$$c_2 = -3w_0 + \frac{9w_{0.5} - 3}{4}. \quad (15)$$

This way, we move on to a scenario in which w_0 and $w_{0.5}$ are the parameters subject to estimation, which can be explicitly reconstructed using Eq. (5):

$$X(z) = (1+z)^{\frac{3}{2}(-8w_0+9w_{0.5}+1)} e^{\left(\frac{3z(w_0(52z+40)-9w_{0.5}(5z+4)+7z+4)}{8(1+z)^2}\right)}, \quad (16)$$

which consistently comes down to the Λ CDM case for $w_0 = w_{0.5} = -1$.

For completeness and purposes related to model selection, it is convenient to compute an effective w_a parameter for this model. By analogy with the CPL case we define

$$w_a = \lim_{z \rightarrow \infty} w(z) - w_0, \quad (17)$$

so in this case

$$w_a = -5w_0 + \frac{9}{2}w_{0.5} - \frac{1}{2} \quad (18)$$

is the result we get.

2.3.2 Chebychev polynomial parametrization

Now we want to make a further generalisation in the fashion of our general proposal above, by considering a bit more involved functions. In this case we make use of Chebychev polynomials (of the first kind), which have a significant role in most areas of numerical analysis, as well as in other areas of Mathematics (polynomial approximation, numerical integration, and pseudo spectral methods for partial differential equation, etc.)

Once again we have to take into account that we can not constrain accurately more than two dark energy parameters (Linder & Huterer 2005), thus we have cut the expansion at the second order. Specifically we propose

$$w(z) = -1 + c_1 T_1(1 + f(z)) + c_2 T_2(1 + f(z)), \quad (19)$$

with T_n being the first kind Chebyshev polynomial of degree n and $f(z) = z/(1+z)$ as before. A convenient presentation of that parametrization is

$$w(z) = -1 + c_1 \left(\frac{1+2z}{1+z}\right) + c_2 \left[2 \left(\frac{1+2z}{1+z}\right)^2 - 1\right]. \quad (20)$$

In this case too we switch to more amenable parameters and then let

$$c_1 = \frac{1}{11}(23w_0 - 9w_{0.5} + 14) \quad (21)$$

$$c_2 = -\frac{3}{11}(4w_0 - 3w_{0.5} + 1). \quad (22)$$

Then, one should simply resort to Eq. (5) to produce the whole scenario:

$$X(z) = (1+z)^{-\frac{3}{4}(52w_0-45w_{0.5}+7)} e^{\left(\frac{3z(w_0(68z+56)-9w_{0.5}(6z+5)+14z+11)}{4(1+z)^2}\right)}. \quad (23)$$

For this first attempt at depicting a dark energy dominated universe with Chebyshev polynomials in terms of those functions we choose w_0 and $w_{0.5}$ as our parameters, but it would be not surprising than one could do better if some extra work was done in the direction of making parameter correlation smaller. For the time being we just pursue to compare directly our polynomial proposal with a preferred presentation of the CPL parametrization on the one hand and with our conventional polynomial proposal on the other hand.

In that direction and as it has been done before, we compute an effective w_a parameter which in this case takes the form

$$w_a = \frac{1}{11}(-49w_0 + 45w_{0.5} - 4). \quad (24)$$

2.3.3 Some additional remarks

In the first place, these two new routes can be viewed as perturbations of Λ CDM, particularly, at low redshifts, which is the region most accurately described by the current data. If one wants to perturb Λ CDM in either the CPL or the Wang scenarios w_0 has to be anchored at -1 and then there is only one free parameter to play with. In contrast, our two new models may model two-parametric departures from Λ CDM, and thus have more flexibility in principle.

Note that it would be possible to consider the two new parametrizations along with CPL(Wang) if one let the parameter space have one more dimension. Indeed, if we let our parametrization be of the form

$$w(z) = b_1 + b_2 \left(\frac{1+2z}{1+z}\right) + b_3 \left(\frac{1+2z}{1+z}\right)^2, \quad (25)$$

then our conventional polynomial case would be obtained for $b_1 = -1$, $b_2 = c_1$, and $b_3 = c_2$; the Chebyshev case would follow from the choice $b_2 = c_1$, $b_3 = 2c_2$ and $b_1 = -(1+c_2)$; and finally the CPL case would be obtained from $b_1 = w_0 - w_a$, $b_2 = w_a$ and $b_3 = 0$.

3 OBSERVATIONAL DATA

As dark energy is expected to have started to dominate at recent times, low redshift datasets are the obvious choice to put the tighter constraints on each dynamics, whereas high redshift ones may be viewed as complementary. Thus the combination of SN and BAO datasets, given their quality in both cases, and the considerable number of data points in the case of the SN, is an excellent choice given the state of the art. Besides, new avenues on BAO (Bassett & Hlozek 2010) are to be open soon which will allow to exploit the tremendous potential of this new astronomical tool towards constraining the main evolutionary features of dark energy. As we have already mentioned, one of our objectives is to introduce new promising parametrizations as alternatives to one of the commonest, but one of the other objectives is to forecast how the old parametrizations and our challengers will cope with new data.

The literature provides a large number of papers where simulated supernovae data are used in the way we have just mentioned, but to our knowledge synthetic baryon acoustic oscillations data have only been presented and exploited in (Escamilla-Rivera et al. 2011). This builds on considerable theoretical efforts in different forecast aspects (Blake et al. 2006), which have crystallized in the package Initiative for Cosmology (iCosmo) (see (Refregier et al. 2011)) and its BAO modules, which have allowed us to produce these mock data. We have modified and extended this general purpose software to produce mock data from a line of sight, high-precision BAO spectroscopic survey as the one described in (Percival 2010; EUCLID EUCLID) and pre-WFIRST supernovae data.

3.1 Baryon Acoustic Oscillations

Baryon Acoustic Oscillations (BAO) have emerged as a promising standard ruler in cosmology, enabling precise measurements of the dark energy parameters with a minimum of systematic errors (Wang et al. 2010; Blake et al. 2006). These oscillations were originated before recombination due to the density fluctuations created by acoustic waves generated by primordial perturbations. After recombination, photons decoupled and propagated freely leaving a signature of the primordial perturbations in the CMB temperature distribution. A similar but attenuated feature appears in the clustering of matter; the peaks and troughs of the acoustic waves gave rise to overdense regions of baryonic matter which imprint a correlation between matter densities at the scale of the sound horizon at recombination

$$r_s(z_r) = \int_{z_r}^{\infty} \frac{c_s(z)}{H(z)} dz, \quad (26)$$

where c_s is the sound speed (Bassett & Hlozek 2010; Percival 2006). Cosmological Microwave Background (CMB) anisotropies provide an absolute physical scale for these baryonic peaks, but these features can be also determined in a galaxy survey. By comparison of the absolute value given by CMB and the observed location of the peaks of the two-point correlation function of the matter distribution, $\xi(z)$ given by a galaxy survey, one can obtain measurements of cosmological distance scales. Measuring the BAO scale from galaxy clustering in the transverse and radial directions

yields measurements of $r(z)/r_s(z_r)$ and of $r_s(z_r)H(z)$ (Blake & Glazebrook 2003; Hu & Haiman 2003; Seo & Eisenstein 2003), where

$$r(z) = \int_0^z \frac{cdz'}{H(z')} \quad (27)$$

is the comoving distance at redshift z .

3.1.1 Percival et al.

In (Percival W. et al. 2010) Gaussian values on the distance ratio, $r_s(z_{\text{drag}})/D_V(z)$, at redshifts $z = 0.2$ and $z = 0.35$, are given from the measures obtained by combining the spectroscopic Sloan Digital Sky Survey (SDSS) and the Two-Degree Field Galaxy Redshift Survey (2DFGRS) data. This distance ratio represents the comoving sound horizon at the baryon dragging epoch, z_{drag} ,

$$r_s(z_{\text{drag}}) = c \int_{z_{\text{drag}}}^{\infty} \frac{c_s(z)}{H(z)} dz, \quad (28)$$

over the effective distance $D_V(z)$, defined as (Eisenstein et al. 2005) as

$$D_V(z) = \left[(1+z)^2 D_A^2(z) \frac{cz}{H(z)} \right]^{1/3}, \quad (29)$$

D_A being the angular diameter distance which takes the form

$$D_A(z) = \frac{c}{1+z} \int_0^z \frac{dz'}{H(z')}, \quad (30)$$

in a flat universe containing only matter and dark energy.

In order to estimate the dark energy parameters in the context of Bayesian statistics, as detailed in Appendix A, we need a definition of the χ^2 which reflects the difference between the observational data and the values given by our models. In our case this requires giving an expression for the comoving sound horizon at the baryon dragging epoch, and we have used the fitting formula proposed in (Eisenstein & Hu 1998):

$$r_s(z_{\text{drag}}) = 153.5 \left(\frac{\Omega_b h^2}{0.02273} \right)^{-0.134} \left(\frac{\Omega_m h^2}{0.1326} \right)^{-0.255}. \quad (31)$$

Now, taking into account the Gaussian values at $z = 0.2$ and 0.35 from the BAO data in (Percival W. et al. 2010), we can calculate

$$\chi_{\text{BAO}}^2 = (v_i - v_i^{\text{BAO}})(C^{-1})_{ij}^{\text{BAO}}(v_j - v_j^{\text{BAO}}) \quad (32)$$

where

$$\mathbf{v} = \left\{ \frac{r_s(z_{\text{drag}}, \Omega_m, \Omega_b; \boldsymbol{\theta})}{D_V(0.2, \Omega_m; \boldsymbol{\theta})}, \frac{r_s(z_{\text{drag}}, \Omega_m, \Omega_b; \boldsymbol{\theta})}{D_V(0.35, \Omega_m; \boldsymbol{\theta})} \right\}, \quad (33)$$

$$\mathbf{v}^{\text{BAO}} = (0.1905, 0.1097) \quad (34)$$

and

$$\mathbf{C}^{-1} = \begin{pmatrix} 30124 & -17227 \\ -17227 & 86977 \end{pmatrix}, \quad (35)$$

being the inverse of the covariance matrix.

3.1.2 High precision spectroscopic redshift surveys

Future BAO surveys are expected to represent a real breakthrough in our knowledge of the dark energy. In (Percival 2010; EUCLID EUCLID) is proposed a survey to measure spectroscopic redshifts for 6.1×10^7 luminous galaxies and clusters of galaxies out to redshift $z = 2$ over 20000 deg^2 , reaching a $dz/(1+z) < 0.001$, enough to resolve the BAO feature along the line of sight, and achieving much better dark energy constraints than their predecessors.

We have used the Initiative for Cosmology (iCosmo) software package to generate the BAO mock data. In this case are concerned with the following two signatures of the BAO peak:

$$y(z) = \frac{r(z)}{r_s(z_r)}, \quad (36)$$

$$y'(z) = \frac{r'(z)}{r_s(z_r)} = \frac{c/H(z)}{r_s(z_r)}. \quad (37)$$

The publicly available code has built-in routines based on the universal BAO fitting formulae for the diagonal errors on y and y' presented in (Blake et al. 2006). Once we have made the proper modifications of the code to replace the defaults (Peacock and Dodds (Peacock & Dodds 1996) power spectrum and Smail et al. (Smail et al. 1994) galaxy distribution) with the survey properties (those quoted above and besides $z_{med} \sim 0.46$, redshift range $0.1 < z < 0.9$), we have written extra codes to generate a large number of normal random realizations around a fiducial model which is specifically the $wcdm+sz+lens$ case from WMAP7-year (Komatsu et al. 2011), which has $\Omega_m = 0.26 \pm 0.099$ and is phantom-like with $w = -1.12 \pm 0.43$. Then after some reduction the synthetic BAO data presented in table 1 have been obtained. In addition, in the the corresponding χ^2 we have introduced priors based on the values of the matter and baryon density presented in (Burigana et al. 2010) as a forecast analysis of Planck: using the result $\Omega_m h^2 = 0.1308 \pm 0.0008$ we construct a weak Gaussian prior, whereas with $\Omega_b h^2 = 0.0223$ we construct a fixed prior. In both cases we use $h = 0.742$ as is given by (Riess et al. 2009). See as well Fig. 1 for a graphical account of the features of our BAO simulated data.

In this case we need an expression for the sound horizon at recombination to constrain the dark energy parameters:

$$r_s(a_r) = \frac{c}{\sqrt{3}H_0\Omega_m^{1/2}} \int_0^{a_r} \frac{da}{(a+a_{eq})^{1/2}} \frac{1}{(1+R)^{1/2}}, \quad (38)$$

which can be evaluated as described in (Efstathiou & Bond 1999) and gives

$$r_s(a_r) = \frac{4000}{\sqrt{\Omega_b h^2}} \frac{\sqrt{a_{eq}}}{\sqrt{1+\eta_\nu}} \ln \left\{ \frac{[1+R(z_r)]^{1/2} + [R(z_r) + R_{eq}]^{1/2}}{1 + \sqrt{R_{eq}}} \right\} \text{Mpc} \quad (39)$$

where $\eta_\nu = 0.6813$ is the ratio of the energy density in neutrinos to the energy in photons. The parameter $R = 3\rho_b/4\rho_\gamma$ is numerically obtained

$$R(a) = 30496\Omega_b h^2 a. \quad (40)$$

The scale factor at which radiation and matter have equal densities is

$$a_{eq}^{-1} = 24185 \left(\frac{1.6813}{1+\eta_\nu} \Omega_m h^2 \right), \quad (41)$$

and the redshift of recombination z_r is given by (Hu & Sugiyama 1996) in the following fitting formula

$$z_r = 1048 (1 + 0.00124(\Omega_b h^2)^{-0.738}) (1 + g_1 (\Omega_m h^2)^{g_2}), \quad (42)$$

being

$$g_1 = 0.0783(\Omega_b h^2)^{-0.238} (1 + 39.5 (\Omega_b h^2)^{0.763})^{-1}, \quad (43)$$

and

$$g_2 = 0.560 (1 + 21.1(\Omega_b h^2)^{1.81})^{-1}. \quad (44)$$

The χ^2 function for BAO mock data is now defined in Eq. 45, where N_{mode} is the number of mock data, in this case 4. And $\theta = \theta_1, \theta_2, \dots$ are the dark energy model parameters. Here we have conveniently accounted for the slight degree of correlation existing between y and y' , and as suggested in (Seo & Eisenstein 2007) we will fix for our calculations $\rho_{y,y'} = 0.4$.

3.2 Type Ia Supernovae

Type Ia supernovae (SN) are the explosions that take place at late stages of the stellar evolution. They have been recognized as a powerful probe of cosmological dynamics, as they give a good measure of the cosmological expansion rate. Supernovae provided the first probe for the cosmological expansion (Riess et al. 1998; Perlmutter et al. 1999) and are considered as standard candles (Leibundgut 2001).

The statistical analysis of such SN samples rests on the definition of the modulus distance:

$$\mu(z_j) = 5 \log_{10}[d_L(z_j, \theta)] + \mu_0, \quad (46)$$

where $d_L(z_j, \theta)$ is the luminosity distance:

$$d_L(z, \theta) = (1+z) \int_0^z dz' \frac{1}{H(z', \theta)}. \quad (47)$$

The best fits for the parameters of a given model can be obtained by minimizing

$$\chi_{\text{SN}}^2(\mu_0, \theta) = \sum_{j=1} \frac{(\mu_{\text{th}}(z_j; \mu_0, \theta) - \mu_{\text{obs}}(z_j))^2}{\sigma_{\mu,j}^2}, \quad (48)$$

where $\sigma_{\mu,j}$ are the measurement variances. Here we have neglected correlations between measurements at different redshifts, as they are typically small; as it is well known, doing this just induces a slight degradation in the constraints, and therefore it is simply a conservative and acceptable procedure.

In our χ_{SN}^2 we have a nuisance parameter, μ_0 , which encodes the Hubble parameter and the absolute magnitude M , and has to be marginalized over. However, when one works with an homogeneous data sample (Nesseris & Perivolaropoulos 2004), an alternative method is used for that purpose. This method consists in maximizing the likelihood by minimizing χ^2 with respect to μ_0 (Elgaroy & Maltamaki 2006). Then one can rewrite the $\chi_{\text{SN}}^2(\mu_0, \theta)$ as

$$\chi_{\text{SN}}^2(\theta) = c_1 - 2c_2\mu_0 + c_3\mu_0^2 \quad (49)$$

being

$$c_1 = \sum_{j=1} \frac{(\mu_{\text{obs}}(z_j) - 5 \log_{10} d_L(z_j; \theta))^2}{\sigma_{\mu,j}^2} \quad (50)$$

$$\chi_{\text{BAO}}^2(\boldsymbol{\theta}) = \frac{1}{1 - \rho_{y,y'}^2} \left[\sum_{j=1}^{N_{\text{mock}}} \frac{(y(z_j, \Omega_m, \Omega_b; \boldsymbol{\theta}) - y_{\text{mock}}(z_j))^2}{\sigma_{y,j}^2} + \sum_{j=1}^{N_{\text{mock}}} \frac{(y'(z_j, \Omega_m, \Omega_b; \boldsymbol{\theta}) - y'_{\text{mock}}(z_j))^2}{\sigma_{y',j}^2} - 2 \rho_{y,y'} \sum_{j=1}^{N_{\text{mock}}} \frac{(y(z_j, \Omega_m, \Omega_b; \boldsymbol{\theta}) - y_{\text{mock}}(z_j))(y'(z_j, \Omega_m, \Omega_b; \boldsymbol{\theta}) - y'_{\text{mock}}(z_j))}{\sigma_{y,j} \sigma_{y',j}} \right] \quad (45)$$

Table 1. Mock BAO data from

z	y	y'
0.6	15.005 ± 0.117	21.401 ± 0.291
0.8	19.221 ± 0.109	18.953 ± 0.186
1.0	22.708 ± 0.102	17.012 ± 0.137
1.2	25.762 ± 0.098	15.098 ± 0.101
1.4	28.635 ± 0.096	13.421 ± 0.079
1.6	31.126 ± 0.101	12.213 ± 0.069
1.8	33.540 ± 0.107	10.987 ± 0.061
2.0	35.357 ± 0.112	10.094 ± 0.055

$$c_2 = \sum_{j=1} \frac{\mu_{\text{obs}}(z_j) - 5 \log_{10} d_L(z_j; \boldsymbol{\theta})}{\sigma_{\mu,j}^2} \quad (51)$$

$$c_3 = \sum_{j=1} \frac{1}{\sigma_{\mu,j}^2} \quad (52)$$

With the minimization over μ_0 one obtains an expression in terms of c_2 and c_3 :

$$\mu_0 = c_2/c_3, \quad (53)$$

so the χ^2 function takes the form

$$\tilde{\chi}_{\text{SN}}^2(\boldsymbol{\theta}) = c_1 - \frac{c_2^2}{c_3}. \quad (54)$$

3.2.1 Union2

Union2 (Amanullah et al. 2010) is one of the largest type Ia Supernovae samples up to date, and it consists of 557 SNIa and covers a redshift range from 0 to 1.4. This sample has increased the number of well-measured Type Ia supernovae of the previous Union (Kowalski et al. 2008) at high redshifts by the combination of different data sets. The Union Sample has been extended with six type Ia supernovae presented in (Amanullah et al. 2010), the SNe from (Amanullah et al. 2008), the low- z and intermediate- z data from (Hicken et al. 2009) and (Holtzman et al. 2008) respectively.

This sample has been obtained after some improvements in the Union analysis chain: all light curves have been fitted using a single light curve fitter (SALT2) to eliminate differences and systematic errors have been directly computed using the effect they have on the distance modulus.

3.2.2 Mock data for a pre-WFIRST stage

To create SN mock samples we have reproduced the pre-WFIRST observational simulation as reported in (Albrecht et al. 2009), which has two population peaks, one at $z < 0.1$ and the other at $0.6 < z < 0.7$; along with a very scarce

population at $z > 1.6$. Specifically, the redshift distribution suggested in (Albrecht et al. 2009) is reproduced here in Table 2.

The formulae for errors on SN magnitudes that we use follows from a prescription used in the binning approach (Kim et al. 2004; Upadhye et al. 2005; Ishak 2007), in which they are calculated as follows:

$$\sigma_m^{\text{eff}} = \sqrt{\sigma_{\text{int}}^2 + \sigma_{\text{pec}}^2 + \sigma_{\text{sys}}^2}, \quad (55)$$

where:

- $\sigma_{\text{int}} = 0.15$ is the intrinsic dispersion in magnitude per SN, assumed to be constant and independent of redshift for all well-designed surveys;
- $\sigma_{\text{pec}} = 5\sigma_v/(\ln(10)cz)$ is the error due to the uncertainty in the SN peculiar velocity, with $\sigma_v = 500$ km/s, c is the velocity of light and z is the redshift for any SN;
- $\sigma_{\text{sys}} = 0.02(z/z_{\text{max}})$ is the floor uncertainty related to all the irreducible systematic errors with cannot be reduced statistically by increasing the number of observations. The value 0.02 is conservative from the perspective of what space-based missions could achieve. Those are precisely the resources expected to provide high-redshift SN, which are in turn the ones in which the systematic error term is expected to contribute. Note as well that z_{max} is the maximum observable redshift in the considered mission and this linear term in redshift is used to account for the dependence with redshift of many of the possible systematic error sources (for example the Malmquist bias or gravitational lensing effects).

We have included some extra (though very slight) noise, and then we have checked that our mock data are compliant with the main features of the Union2 sample. The fiducial model used is again the Λ CDM+ z +lens case from WMAP7-year as quoted above, which has $\Omega_m = 0.26 \pm 0.099$ and is phantom-like with $w = -1.12 \pm 0.43$. The χ^2 function for the SN mock data has been constructed as described in Sec. (3.2). Then we have let *iCosmo* generate the d_L values for the redshifts in the table a large number of universes drawn randomly and

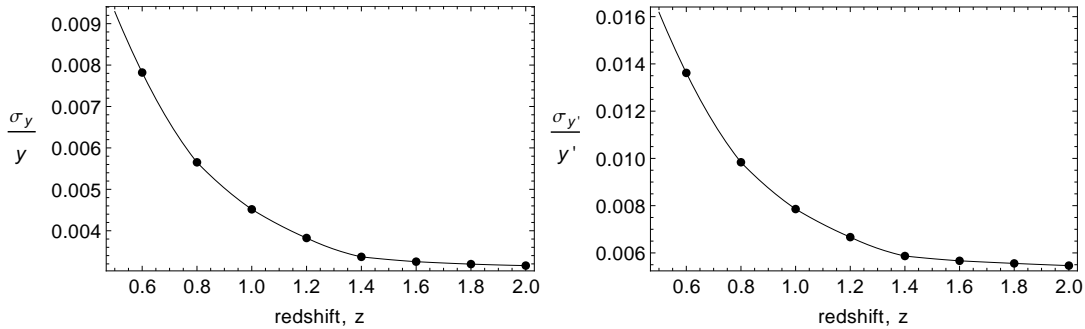


Figure 1. Fractional errors on synthetic BAO data for y (a) and y' (b).

Table 2. Redshift distribution of pre-WFIRST SN samples

redshift bin	# of SN
< 0.1	500
0.1 – 0.2	200
0.2 – 0.3	320
0.3 – 0.4	445
0.4 – 0.5	580
0.5 – 0.6	660
0.6 – 0.7	700
0.7 – 0.8	670
0.8 – 0.9	110
0.9 – 1.0	80
1.0 – 1.1	25
1.1 – 1.2	16
1.2 – 1.3	16
1.3 – 1.4	4
1.4 – 1.5	4
1.5 – 1.6	4
> 1.6	4

normally distributed around the fiducial one, and finally we have performed a reduction to give our mock sample.

4 RESULTS

Following Bayesian Statistics, we have inferred the values Ω_m and the dark energy parameters for the models considered. For further details see A. We report our findings in two main ways: on the one hand we present our best fits, errors and derived quantities in Tables 3, 4; on the other hand we present credible contours obtained after a numerical marginalization over Ω_m , where we have approximate the likelihood as a Gaussian and then analytically marginalize, see (Taylor & Kitching 2010) and references therein. As mentioned, we have considered the combination of real and mock SN and BAO data as discussed above, and in addition we have introduced in all cases a Gaussian prior on Ω_m and Ω_b deduced in (Burigana et al. 2010) as a forecast analysis of Planck: $\Omega_m h^2 = 0.1308 \pm 0.0008$, $\Omega_b = 0.0223$ with $h = 0.742$ as is given by (Riess et al. 2009).

The presence of the prior leads to uniformity in the best fit value of Ω_m thus minorating its influence in the dark energy constraints. This trick, together with the marginalization, allow to focus the discussion on the dark energy parameters thus offering a clearer picture of what each parametrization can offer.

Let us now examine our results using different criteria. First of all uncertainties in percentage terms on the dark energy values can be considered. The conventional polynomial turns out to give the lowest percentage error on w_0 for both current and recent data, and the second best is the Chebyshev setting, although we only get a marginal difference with respect to the conventional polynomial and Wang’s model. The situation gets reversed, though, for the percentage error on $w_{0.5}$, and Wang’s parametrization is the best performer, but again differences are small when compared to our parametrizations (CPL gets excluded from this discussion item as the parameter $w_{0.5}$ is not considered).

Note that the substantial reduction on percentual errors when one moves from current to mock data, typically they become almost three times smaller. Up to some degree this may be a consequence of the use of a fiducial model in the simulated data, probably real future data will be significantly better than current ones but perhaps not as remarkably as our synthetic data.

Summarizing, this section of the analysis, we see that in general choosing w_0 and $w_{0.5}$ as the parameters to constrain is worthy as percentual errors are low. In our two new parametrizations are indeed valuable from this particular perspective, but are they as valuable when one considers other criteria?

Another interesting point of view to interpret our re-

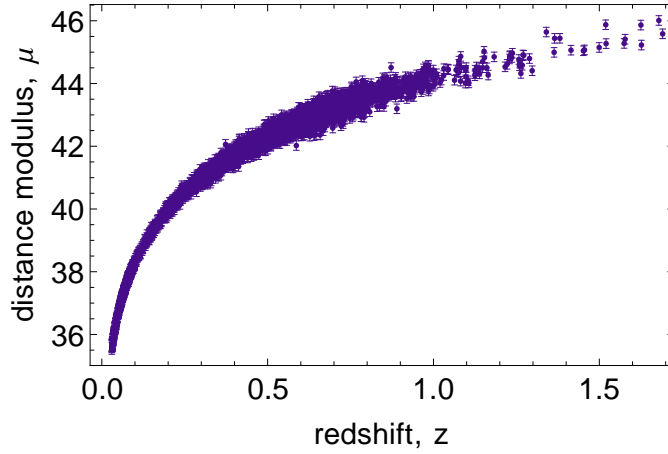


Figure 2. Mock data obtained with iCosmo for the pre-WFIRST specifications.

Table 3. Constraints on dark energy parameters and derived quantities from current data.

Model	χ^2_{min}	Ω_m	Dark energy parameters	FoM _{Wang} (FoM _{DETF})	$\rho_{1,2}$	DIC
CPL	544.91	0.315 ± 0.033	$w_0 = -1.033 \pm 0.180$ $w_a = -0.742 \pm 1.520$	14.16 (14.16)	-0.930	10.30
Wang	544.91	0.315 ± 0.033	$w_0 = -1.033 \pm 0.180$ $w_{0.5} = -1.281 \pm 0.361$	42.47 (14.16)	-0.792	8.11
Chebyshev Polynomial	544.96	0.314 ± 0.032	$w_0 = -1.049 \pm 0.163$ $w_{0.5} = -1.268 \pm 0.373$	43.63 (11.67)	-0.785	8.02
Conventional Polynomial	544.98	0.314 ± 0.032	$w_0 = -1.055 \pm 0.157$ $w_{0.5} = -1.263 \pm 0.377$	44.11 (9.80)	-0.780	7.98

sults is Pearson’s correlation coefficient (for the dark energy), defined as

$$\rho_{1,2} = \frac{\sigma_{12}^2}{\sigma_1 \sigma_2} \quad (56)$$

which can be used to study the lineal correlation between either two dark energy parameters. Here σ_{12} stands generically for the non-diagonal element of the covariance matrix for the parameters 1 and 2. A value of $\rho_{1,2}$ close to zero will tell us there is no linear correlation between them, and lowering correlation typically improves constraints, so if a given parametrization achieves that goal naturally then it will most likely provide an overall worthy scenario.

A related magnitude is the (frequentist) Figure-of-Merit (FoM), which has been defined in two slightly different but related ways in the literature. We present both and discuss their specific features and report their values for the benefit of the readers keener to one version or the other. Following the corresponding references we use subscripts to differentiate them. According to (Wang 2008)

$$\text{FoM}_{\text{Wang}} = \frac{1}{\sqrt{\det \mathbf{C}(c_1, c_2, c_3, \dots)}}, \quad (57)$$

where $\mathbf{C}(c_1, c_2, c_3, \dots)$ is the covariance matrix of the corresponding c_i dark energy parameters one is concerned with.

As explained in (Wang 2008), this specific definition has two advantages: firstly it is easy to calculate for either real or simulated data, and secondly it has an easy physical interpretation. The FoM penalizes experiments that yield very correlated estimates for the dark energy parameters. Hence the FoM is larger when the dark energy parameters c_i are chosen such that they are minimally correlated with each other. But obviously, if the model considered does not have a low degree of correlation *per se* one will be giving a poor estimation of the performance of the observational tests.

A closely related, and perhaps more popular version of the FoM was proposed by the “Dark Energy Task Force” (see (Albrecht et al. 2009) for a recent revision of the topic), and it simply reads

$$\text{FoM}_{\text{DETF}} = \frac{1}{\sqrt{\det \mathbf{C}(w_0, w_a)}}. \quad (58)$$

Thus, the main difference with respect to the FoM_{Wang} is that in this view the two relevant parameters are w_0 and w_a , and not any others. However, w_a is a parameter informing about early asymptotics, which is a region with extremely hard observational access and physical interpretation, and thus, the debate persists of whether a FoM using that parameter may not be given artificially large results.

Table 4. Constraints on dark energy parameters and derived quantities from simulated data.

Model	χ^2_{min}	Ω_m	Dark energy parameters	FoM _{Wang} (FoM _{DETF})	$\rho_{1,2}$	DIC
CPL	5320.38	0.269 ± 0.005	$w_0 = -1.151 \pm 0.041$ $w_a = 0.244 \pm 0.207$	616.25 (616.25)	-0.946	21.44
Wang	5320.38	0.269 ± 0.005	$w_0 = -1.151 \pm 0.041$ $w_{0.5} = -1.069 \pm 0.031$	1848.70 (616.25)	-0.712	11.69
Chebyshev polynomial	5320.43	0.269 ± 0.005	$w_0 = -1.140 \pm 0.035$ $w_{0.5} = -1.073 \pm 0.029$	2065.28 (504.85)	-0.666	11.38
Conventional polynomial	5320.45	0.269 ± 0.005	$w_0 = -1.137 \pm 0.033$ $w_{0.5} = -1.075 \pm 0.028$	2147.57 (477.24)	-0.648	11.29

According to Appendix C, the two FoMs are linearly related:

$$\text{FoM}_{\text{DETF}} = m_3 \text{FoM}_{\text{Wang}} \quad (59)$$

with $m_3 = 1/3, 2/9, 11/45$ for Wang, Chebyshev polynomial, Conventional polynomial models respectively.

Our results on the FoM get summarized very simply: the conventional polynomial has the largest value of the FoM_{Wang}, whereas the results get complete reversed for the FoM_{DETF}. In addition, the ratios between the different FoMs are very similar for real and synthetic data. However, as follows from our discussion before, the price paid to get a larger FoM (by a redefinition) it to waive the importance of correlation, and further investigations and reflections would be needed to provide a definite solution to this debate, which is, on the other hand, out of the scope of this paper.

For both sorts of data the conventional polynomial parametrization is naturally less correlated than all three others. The second best is the Chebyshev one, and all three are considerably less correlated than CPL. Nevertheless, even though Wang's second parameter $w_c \equiv w_{0.5}$ is chosen for the low degree of correlation with w_0 , a better choice for that purpose would be the dark energy EOS parameter evaluated at a lower redshift (say $z \sim 0.25$). This was already pointed out in (Wang 2008) and confirmed in (Escamilla-Rivera et al. 2011). In agreement with our discussion the degree of correlation at a certain low redshift in our two new parametrizations immediately drives to very narrow errors on the total w at that location, as reflected in Fig. 3, where we represent the total w for our best fits and the 1σ error bands. In fact these two figures serve the additional purpose of illustrating the sort of evolution described our parametrizations. Nevertheless, as correlation is a topic worth of further consideration we elaborate in Appendix B.

Finally, the last criterion we resort to is the Bayesian deviance information criterion (DIC). This is a very interesting way to examine results in this context, in particular when one finds marginal differences in the χ^2 values. This criterion accounts for the dependence of χ^2 on our parameters, but it also somehow involves the correlation and the percentual errors, thus turning out to be far more informative and having more discerning power. When applied for model selection, as we put forward, the setting with the

lowest DIC is in principle the best. In our case, as we are mainly concerned with dark energy issues given that Ω_m is very tightly constrained we construct our DIC starting from a χ^2 marginalized over Ω_m . Namely

$$\text{DIC} = 2\overline{\chi^2(\boldsymbol{\theta})} - \widehat{\chi^2(\boldsymbol{\theta}_{bf})}, \quad (60)$$

where

$$\widehat{\chi^2} = -2 \log \left(\int_0^1 \exp(-\chi^2/2) d\Omega_m \right). \quad (61)$$

The behaviour of the DIC follows the same pattern as the FoM (although the FoM is not so convenient as a model selection criterion as it does not involve χ^2). Basically, the conventional polynomial model is the best one, then we have the Chebyshev polynomial model, then Wang's scenario, and finally, the CPL model closes the ranking with the highest DIC by far.

Finally, we can see that the FoM values obtained with the mock data are typically better than those for currently available data. This fact proves the capability of the forthcoming surveys to describe the evolutionary features of dark energy.

5 CONCLUSIONS

Parametrizing dark energy in a phenomenological way offers the possibility of progressing in the characterization of this main component of the Universe even though its origin has not been yet unveiled from a theoretical perspective. The extensive prior knowledge available on the topic hints that compliance with relevant astrophysical data favours parametrizations which are smooth and have two parameters only. A second order requirement is restraint at high redshifts in the sense that dark energy should never redshift slower than matter, but neither display an significant blueshift.

Given those guidelines, in this work we present two new polynomial parametrizations of dark energy and we pay attention to some particular aspects which are important for model selection. On the one hand we examine the degree of correlation between the two parameters chosen in our proposal; specifically those are the EOS values at $z = 0$ and

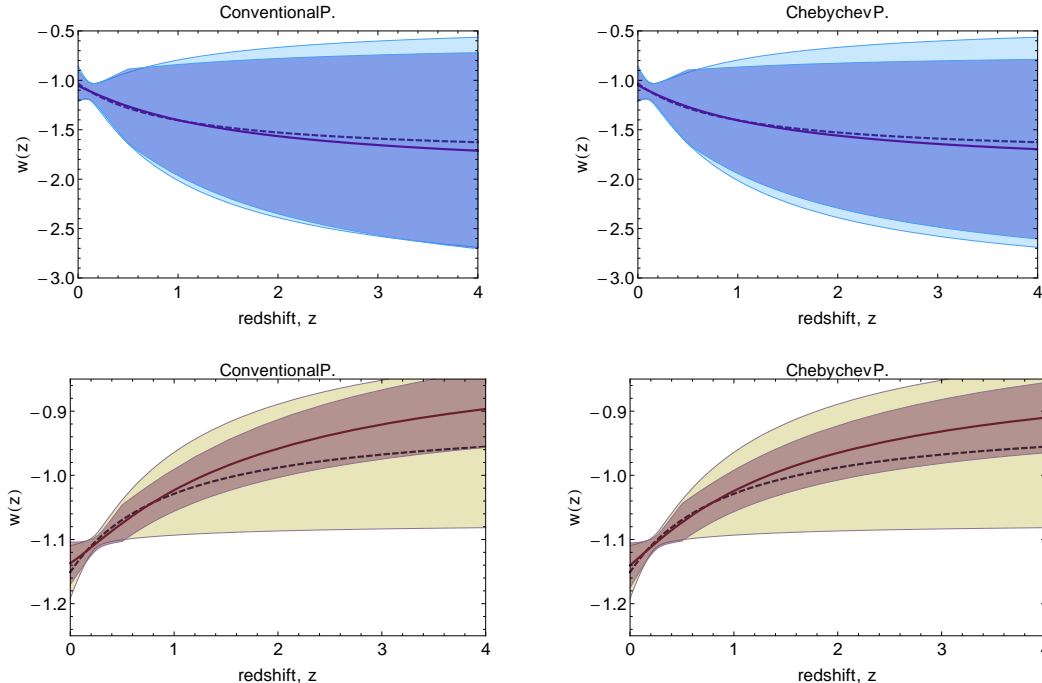


Figure 3. Total w and 1σ error bands for our best fits for real (a) and mock data (b) compared with the results for the CPL parametrization (dashed lines and light contours).

$z = 0.5$, which have been already shown to provide a convenient way to revisit and have already been shown to provide a preferred way to reconsider. On the other hand we resort to a genuinely Bayesian model selection criterion, the deviance information criterion (DIC) for a better account of the improvements that our parametrizations represent.

The astronomical tests we perform make use of SN luminosity data and the typical BAO related scales, so we are focusing on low redshift probes, although our parametrizations are suitable (as they are well behaved at high redshifts) for the analysis of CMB constraints which we hope to address in the future.

The conclusions that emerge from our analysis is that our new parametrizations perform better in the sense that they allow to obtain tighter constraints on the dark energy EOS at present and its derivative, and they are also favoured by the statistical indicator we mention above (DIC). The main reason why we feel they fare better than their competitors is that they represent rather flexible perturbations of the Λ CDM scenario, which in many respects still remains the best description of the accelerated universe, and not surprisingly is often referred to as the concordance model. In contrast, either CPL or Wang are models which when taken as perturbations of Λ CDM are left with one free parameter only, and then one could expect less ability to accommodate themselves to the data.

Note as well that the dataset we consider are not only some currently available, but we also simulate surveys to come, in particular, it is of interest our provision of synthetic measurements of the radial and transversal BAO scales as expected to be obtained with the EUCLID spectroscopic survey, which as expected help us conclude that future surveys will decrease considerably our degree of igno-

rance about dark energy evolution by providing far tighter constraints that may eventually lead to the conclusion that a cosmological constant is not the preferred candidate for the dark energy.

ACKNOWLEDGEMENTS

Throughout this work we have benefited from illuminating conversations with Vincenzo Salzano and Narciso Benítez, and we also acknowledge fruitful exchanges with Adam Amara, Bruce Bassett, Karl Glazebrook, Christopher Gordon, Thomas Kitching, David Parkinson, Anais Rassat, and Yun Wang. Irene Sendra holds a PhD FPI fellowship-contract from the Spanish Ministry of Science and Innovation and Ruth Lazkoz and Irene Sendra are supported by the Spanish Ministry of Science and Innovation through research projects FIS2010-15492, Consolider EPI CSD2010-00064 and also by the Basque Government through the special research action KAFEa during the initial stage of this work.

APPENDIX A: PARAMETER ESTIMATION

The likelihood function, $\mathcal{L}(\mathbf{d}|\boldsymbol{\theta}, \mathcal{M})$, is defined up to proportionality, as the probability of measuring the data $\mathbf{d} = \{d_1, \dots, d_n\}$ given the model \mathcal{M} and its parameters taking the values $\boldsymbol{\theta} = \{\theta_1, \dots, \theta_\nu\}$ (Väliiviita 2005; Denison et al. 2002).

Despite our aim to keep the discussion in this section as general as possible, when we analyse particular datasets we will assume, as usual, that the measurements are normally distributed around their true value, so that

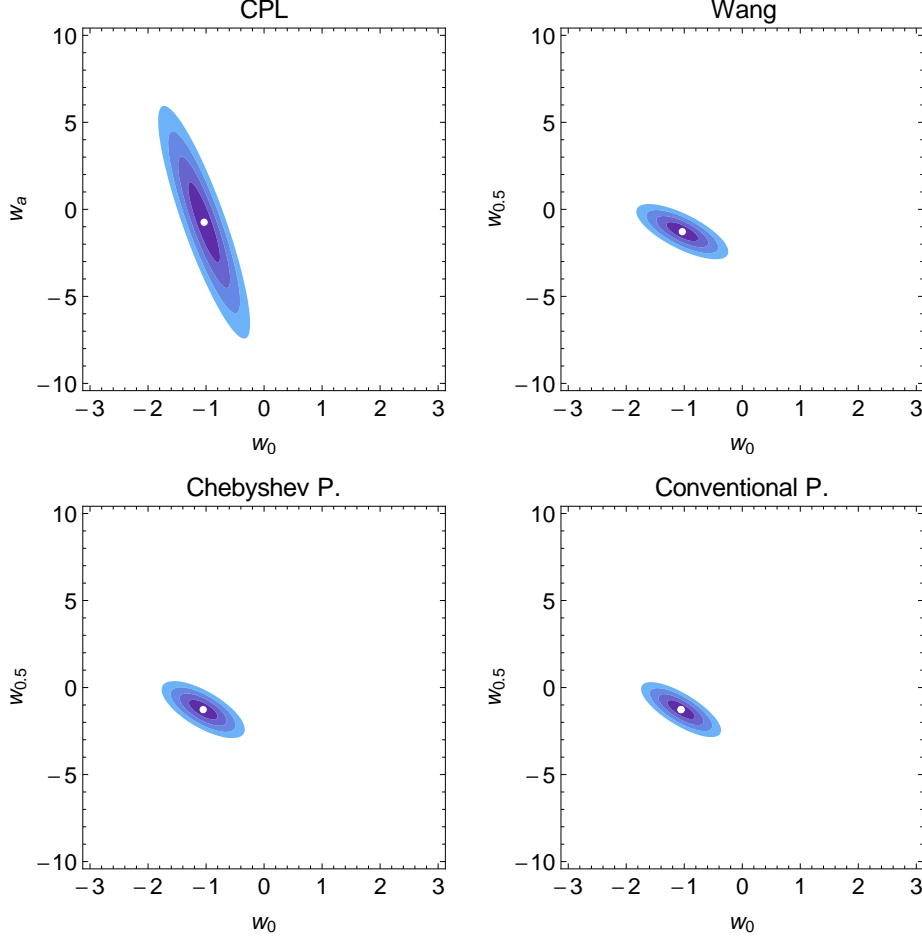


Figure 4. Confidence contours for the four parametrizations using current data.

$$\mathcal{L}(\mathbf{d}|\boldsymbol{\theta}, \mathcal{M}) \propto e^{-\chi^2(\boldsymbol{\theta})/2}. \quad (\text{A1})$$

The probability density function $p(\boldsymbol{\theta}|\mathbf{d}, \mathcal{M})$ of the parameters to have values $\boldsymbol{\theta}$ for the data, \mathbf{d} , under the assumption that the true model is \mathcal{M} is provided by Bayes' theorem (Väliiviita 2005)

$$p(\boldsymbol{\theta}|\mathbf{d}, \mathcal{M}) = \frac{\mathcal{L}(\mathbf{d}|\boldsymbol{\theta}, \mathcal{M})\pi(\boldsymbol{\theta}, \mathcal{M})}{\int \mathcal{L}(\mathbf{d}|\boldsymbol{\theta}, \mathcal{M})\pi(\boldsymbol{\theta}, \mathcal{M})d\boldsymbol{\theta}}, \quad (\text{A2})$$

where $p(\boldsymbol{\theta}|\mathbf{d}, \mathcal{M})$ and $\pi(\boldsymbol{\theta}, \mathcal{M})$ are the posterior and prior probability density functions (pdf) respectively (Väliiviita 2005; Trotta 2004, 2007; Cousins 1995; Denison et al. 2002). The prior pdf encodes all previous knowledge about the parameters before the observational data have been collected. It can be regarded as a subjective procedure, but its use is compulsory in the Bayesian framework, which is the approach used in theoretical frameworks where only one particular realization of the measurement is available.

Parameter estimation in the Bayesian framework is based on maximizing the posterior pdf $p(\boldsymbol{\theta}|\mathbf{d}, \mathcal{M})$, whereas in a “strict” frequentist approach one just maximizes $\mathcal{L}(\mathbf{d}|\boldsymbol{\theta}, \mathcal{M})$. When one uses flat priors in the Bayesian approach then the same conclusions are drawn from both approaches and then the difference turns to be conceptual only (Trotta 2004, 2007, Trotta). If the measured observables are independent from each other and Gaussian distributed around their true value, $\mathbf{d}(\boldsymbol{\theta})$, with a covariance matrix \mathbf{C} ,

given by the experimental errors, maximizing \mathcal{L} is equivalent to minimizing the chi-square function

$$\chi^2(\boldsymbol{\theta}) \equiv \left(\mathbf{d}^{obs} - \mathbf{d}(\boldsymbol{\theta})\right) \mathbf{C}^{-1} \left(\mathbf{d}^{obs} - \mathbf{d}(\boldsymbol{\theta})\right)^T \quad (\text{A3})$$

and for uncorrelated data $C_{ij} = \delta_{ij}\sigma_i^2$,

$$\chi^2(\boldsymbol{\theta}) \equiv \sum_{i=1}^n \left(\frac{d_i^{obs} - d_i(\boldsymbol{\theta})}{\sigma_i^{obs}} \right)^2. \quad (\text{A4})$$

The second step toward constraining parameters satisfactorily is to construct credible intervals (Trotta 2004) which measure the degree of confidence that a certain data was generated by parameters belonging to the estimated interval. which gives the best fit parameters In the Bayesian approach, the credible intervals are drawn around the maximum likelihood point, $\boldsymbol{\theta}_{bf}$. After obtaining it by the minimization of the $\chi^2(\boldsymbol{\theta})$, the boundaries of the region containing 100n% of likelihood are determined as the values of the parameters for which χ^2 has increased by a certain quantity

$$\chi^2 - \chi_{min}^2 = \Delta_{\nu, n} \quad (\text{A5})$$

with

$$n = 1 - \frac{\int_{\Delta_{\nu, n}}^{\infty} t^{\frac{\nu}{2}-1} e^{-t} dt}{\int_0^{\infty} t^{\frac{\nu}{2}-1} e^{-t} dt} = 1 - \frac{\Gamma\left(\frac{\nu}{2}, \frac{\Delta_{\nu, n}}{2}\right)}{\Gamma\left(\frac{\nu}{2}\right)} \quad (\text{A6})$$

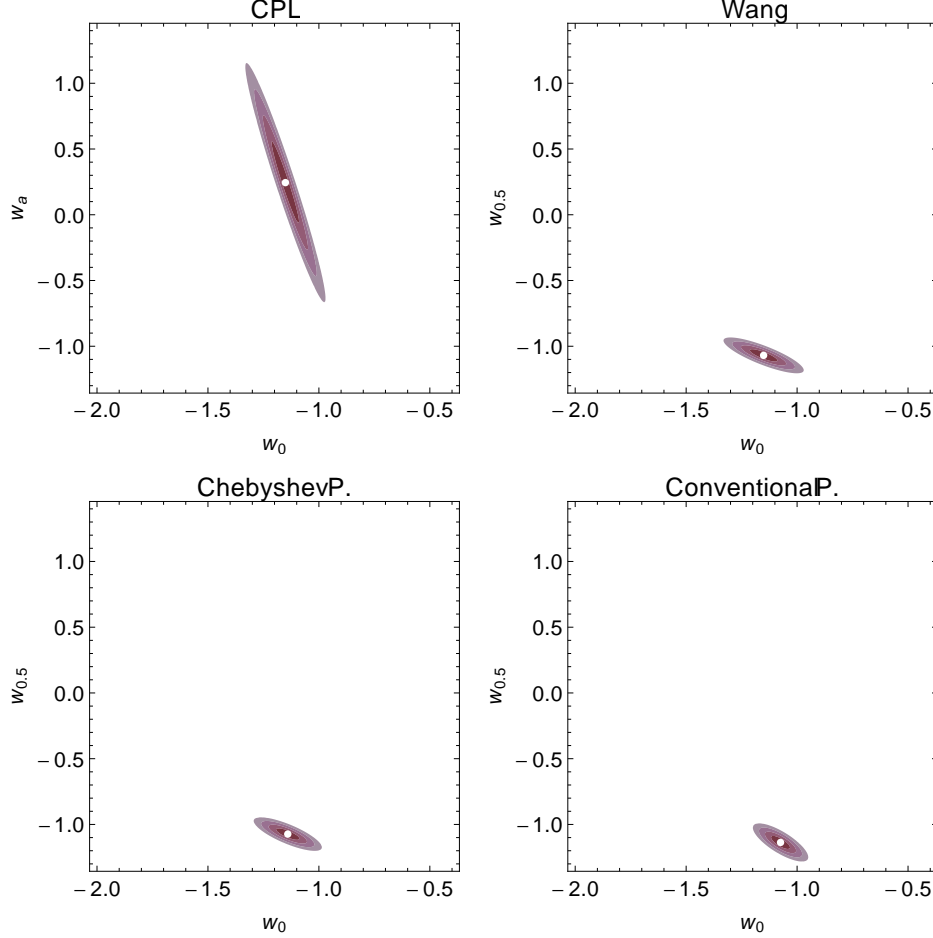


Figure 5. Confidence contours for the four parametrizations using simulated data.

where $\Gamma(\nu/2, \Delta_{\nu,k}/2)$ is the incomplete Γ function (Lazkoz et al. 2005), (Press et al. 1992).

The 1σ and 2σ errors of the parameter θ_i are given by the 68.30% and 95.45% credible interval contours, respectively. The upper limit is the maximum value of the contour and the lower one the minimum one.

APPENDIX B: PIVOT COMPUTATION

B1 Wang's parametrization

The change of variables transforming the CPL parametrization into Wang's is

$$w_c = w_0 + (1 - a_c)w_a, \quad (\text{B1})$$

where w_c is the dark energy parameter EOS at the pivot redshift z_c for which some correlation related (good) feature is achieved. Wang's choice $w_c = 0.5$ leads to a low correlation situation, whereas we are letting w_c stand for the value associated with the lowest correlation possible, so our scope is more general.

Using error propagation one gets

$$\sigma_c^2 = \sigma_0^2 + (1 - a_c)\sigma_a^2 + 2(1 - a_c)\sigma_{12}, \quad (\text{B2})$$

directly from Eq. B1. In the remainder we will drop the absolute value given that we are only interested in a $a_c < 1$

situation. In contrast, if one solves Eq. B1 for w_a and then applies on it error propagation the result

$$\sigma_a^2 = \frac{\sigma_0^2 + \sigma_c^2 - 2\sigma_{0c}}{(1 - a_c)^2} \quad (\text{B3})$$

follows. Combining our results above

$$\sigma_0^2 + (1 - a_c)\sigma_{12} = \sigma_{0c} \quad (\text{B4})$$

is obtained, and then one deduces that total decorrelation ($\sigma_{0c} = 0$) is achieved for

$$a_c = 1 + \sigma_0^2/\sigma_{12}, \quad (\text{B5})$$

which corresponds for our results to $z_c = 0.16, 0.26$ respectively for real and synthetic data. Note that according to our notation σ_{12} denotes in this case the non-diagonal element of the covariance matrix of w_0 and w_a , whereas σ_{0c} denotes the non-diagonal element of the covariance matrix between w_0 and w_c .

But if one is just demanding a situation where $\sigma_{0c} < \sigma_{12}$ it is very easy to deduce from Eq. B4 that such condition is met whenever

$$a_c > \sigma_0^2/\sigma_{12}. \quad (\text{B6})$$

B2 Chebyshev polynomial

Provided $w_{0.5} = w|_{z=0.5}$, let us adopt for w_c the most general definition along the ideas discussed in their previous subsection. For our Chebyshev polynomial parametrization we have

$$w_c = \frac{1}{11} (-6a_c^2(4w_0 - 3w_{0.5} + 1) + a_c(73w_0 - 63w_{0.5} + 10) - 38w_0 + 45w_{0.5} - 4). \quad (\text{B7})$$

Following the same straightforward calculation as for the previous case we conclude there will be minimal correlation for

$$a_c = \frac{\sqrt{729\sigma_{12}^2 - 2142\sigma_{12}\sigma_0^2 + 1681\sigma_0^4 + 63\sigma_{12} - 73\sigma_0^2}}{12(3\sigma_{12} - 4\sigma_0^2)}, \quad (\text{B8})$$

which corresponds to $z_c = 0.17, 0.28$ respectively for real and synthetic data. Sticking to our notation here σ_{12} denotes the non-diagonal element of the covariance matrix of w_0 and $w_{0.5}$, and σ_{0c} has the same meaning as in the case before.

But again one can just want to meet the less restrictive requirement $\sigma_{0c} < \sigma_{12}$, which follows provided

$$(3a_c - 2)(6a_c - 17)\sigma_{12} < (24a_c^2 - 73a_c + 38)\sigma_0^2. \quad (\text{B9})$$

B3 Conventional polynomial

Finally, following the same steps as before, but this time considering the conventional polynomial parametrization we have

$$w_c = \frac{1}{4}(4(2 - 3a_c)(a_c - 2)w_0 + 9(a_c - 2)(a_c - 1)w_{0.5} + (2 - 3a_c)a_c + 3a_c - 2). \quad (\text{B10})$$

The same route as for the two previous cases drives us to the conclusion that the minimal correlation situation is achieved for

$$a_c = \frac{9\sigma_{12} - 8\sigma_0^2}{9\sigma_{12} - 12\sigma_0^2}, \quad (\text{B11})$$

which corresponds to $z_c = 0.18, 0.29$ respectively for real and synthetic data. Here the meaning of σ_{12} and σ_{0c} is exactly the same of the case before.

Finally, one can deduce the condition for the less restrictive requirement $\sigma_{0c} < \sigma_{12}$, to happen is simply

$$\frac{1}{4}(7 - 3a_c)(2 - 3a_c)\sigma_{12} < (2 - 3a_c)(2 - a_c)\sigma_0^2. \quad (\text{B12})$$

APPENDIX C: EQUIVALENCE BETWEEN FOM_{DETF} AND FOM_{WANG}

Following (Coe 2009) we get

$$\mathbf{C}'^{-1} = \mathbf{M}^T \mathbf{C}^{-1} \mathbf{M} \quad (\text{C1})$$

where

$$\mathbf{C} = \begin{pmatrix} \sigma_1^2 & \sigma_{12} \\ \sigma_{12} & \sigma_2^2 \end{pmatrix}. \quad (\text{C2})$$

and $M_{ij} = \partial p_i / \partial p'_j$. In our case $\{p_1, p_2\} = \{w_0, w_{0.5}\}$ and $\{p'_1, p'_2\} = \{w_0, w_a\}$, and specifically $w_{0.5} = m_1 + m_2 w_0 +$

$m_3 w_a$ with m_1, m_2, m_3 coefficients different in the different parametrizations considered other than the CPL one, thus

$$\mathbf{M} = \begin{pmatrix} 1 & 0 \\ m_2 & m_3 \end{pmatrix}. \quad (\text{C3})$$

It is a simple matter of algebra to see that

$$\mathbf{C}' = \begin{pmatrix} \sigma_1^2 & \frac{\sigma_{12} - m_2\sigma_1^2}{m_3} \\ \frac{\sigma_{12} - m_2\sigma_1^2}{m_3} & \frac{m_3}{m_2^2\sigma_1^2 - 2m_2\sigma_{12} + \sigma_2^2} \end{pmatrix} \quad (\text{C4})$$

and $\sqrt{\det \mathbf{C}'} = \sqrt{\det \mathbf{C}}/m_3$. Therefore we get the simple relationship between the two definitions of FoM

$$\text{FoM}_{\text{DETF}} = m_3 \text{FoM}_{\text{Wang}}. \quad (\text{C5})$$

References

- Albrecht A. J., et al., 2009
- Amanullah R., et al., 2008, *A&A*, 486, 375
- Amanullah R., et al., 2010, *ApJ*, 716, 712
- Astier P., et al., 2006, *A&A*, 447, 31
- Bahcall N. A., Bode P., 2003, *ApJ*, 588, L1
- Bahcall N. A., et al., 2003, *ApJ*, 585, 182
- Bassett B. A., Hlozek R., 2010, in Ruiz-Lapuente P., ed., , Dark Energy. Cambridge University Press
- Beaulieu J. P., et al., 2010
- Bento M. C., Bertolami O., Sen A. A., 2002, *Phys. Rev.*, D66, 043507
- Blake C., et al., 2006, *MNRAS*, 365, 255
- Blake C., Glazebrook K., 2003, *ApJ*, 594, 665
- Burigana C., et al., 2010, *ApJ*, 724, 588
- Chevallier M., Polarski D., 2001, *Int. J. Mod. Phys.*, D10, 213
- Coe D., 2009, Arxiv preprint arXiv09064123, pp 2–5
- Cole S., et al., 2005, *MNRAS*, 362, 505
- Cousins R. D., 1995, *Am. J. Phys.*, 63, 398
- Croft R. A. C., Hu W., Dave R., 1999, *Phys. Rev. Lett.*, 83, 1092
- de Bernardis P., et al., 2000, *Nature*, 404, 955
- Denison D. G. T., Holmes C. C., Mallick B. K., Smith A. F. M., 2002, *Bayesian Methods for Nonlinear Classification and Regression*, 1 edn. Wiley
- Efstathiou G., Bond J. R., 1999, *MNRAS*, 304, 75
- Eisenstein D. J., et al., 2005, *ApJ*, 633, 560
- Eisenstein D. J., Hu W., 1998, *ApJ*, 496, 605
- Eke V. R., Cole S., Frenk C. S., Henry J. P., 1998, *MNRAS*, 298, 1145
- Elgaroy O., Multamaki T., 2006, *JCAP*, 0609, 002
- Escamilla-Rivera C., Lazkoz R., Salzano V., Sendra I., 2011, *JCAP*, 1109, 003
- EUCLID, <http://sci.esa.int/euclid>
- Goldstein J. H., et al., 2003, *ApJ*, 599, 773
- Hawkins E., et al., 2003, *MNRAS*, 346, 78
- Hicken M., et al., 2009, *ApJ*, 700, 1097
- Holtzman J. A., et al., 2008, *Astron. J.*, 136, 2306
- Hu W., Haiman Z., 2003, *Phys. Rev.*, D68, 063004
- Hu W., Sugiyama N., 1996, *ApJ*, 471, 542
- Ishak M., 2007, *Found.Phys.*, 37, 1470
- Kim A. G., Linder E. V., Miquel R., Mostek N., 2004, *MNRAS*, 347, 909
- Komatsu E., et al., 2011, *Astrophys. J. Suppl.*, 192, 18

Kowalski M., et al., 2008, ApJ, 686, 749
 Lazkoz R., Nesseris S., Perivolaropoulos L., 2005, JCAP, 2005, 010
 Lechtenfeld O., Popov A. D., Uhlmann S., 2002, Nuclear Physics B, 637, 119
 Leibundgut B., 2001, Ann. Rev. Astron. Astrophys., 39, 67
 Li M., 2004, Phys. Lett., B603, 1
 Linder E. V., 2003, Phys. Rev. Lett., 90, 091301
 Linder E. V., Huterer D., 2005, Phys. Rev. D, 72, 043509
 Maartens R., 2005, AIP Conf.Proc., 736, 21
 McDonald P., et al., 2005, ApJ, 635, 761
 Nesseris S., Perivolaropoulos L., 2004, Phys. Rev., D70, 043531
 Nojiri S., Odintsov S. D., 2006, Phys. Lett., B637, 139
 Peacock J. A., Dodds S. J., 1996, MNRAS, 280, L19
 Percival W., 2006, in Klöckner H. K., Rawlings S., Jarvis M., A. T., eds, Cosmology, Galaxy Formation and Astroparticle Physics on the Pathway to the SKA Baryon acoustic oscillations. ASTRON, p. 187
 Percival W., 2010, <http://sci.esa.int/science-e/www/object/doc.cfm?fobjectid=46450>
 Percival W. W. J., et al., 2010, MNRAS, 401, 2148
 Perlmutter S., et al., 1999, ApJ, 517, 565
 Pope A. C., et al., 2004, ApJ, 607, 655
 Press W., Teukolsky S., Vetterling W., Flannery B., 1992, Numerical Recipes in C, 2nd edn. Cambridge University Press, Cambridge, UK
 Readhead A. C. S., et al., 2004, ApJ, 609, 498
 Refregier A., 2003, Ann. Rev. Astron. Astrophys., 41, 645
 Refregier A., Amara A., Kitching T., Rassat A., 2011, A&A, 528, A33
 Refregier A., et al., 2010
 Riess A. G., et al., 1998, Astron. J., 116, 1009
 Riess A. G., et al., 2004, ApJ, 607, 665
 Riess A. G., et al., 2009, ApJ, 699, 539
 Seo H.-J., Eisenstein D. J., 2003, ApJ, 598, 720
 Seo H.-J., Eisenstein D. J., 2007, ApJ, 665, 14
 Smail I., Ellis R. S., Fitchett M. J., 1994, MNRAS, 270, 245
 Sotiriou T. P., Faraoni V., 2010, Rev. Mod. Phys., 82, 451
 Spergel D. N., et al., 2003, ApJ Suppl., 148, 175
 Spergel D. N., et al., 2007, ApJ Suppl., 170, 377
 Taylor A. N., Kitching T. D., 2010, MNRAS, 408, 865
 Tegmark M., et al., 2004, Phys. Rev. D, 69, 103501
 Trotta R., , private communication
 Trotta R., 2004, PhD thesis, Faculté des sciences de l'Université de Genève
 Trotta R., 2007, MNRAS, 378, 819
 Upadhye A., Ishak M., Steinhardt P. J., 2005, Phys.Rev., D72, 063501
 Väliiviita J., 2005, PhD thesis, Helsinki Institute of Physics
 Van Waerbeke L., et al., 2001, A&A, 374, 757
 Viana P. T. P., Nichol R. C., Liddle A. R., 2002, ApJ, 569, L75
 Wang Y., 2008, Phys. Rev. D, 77, 123525
 Wang Y., Percival W., Cimatti A., Mukherjee P., Guzzo L., et al., 2010, MNRAS, 409, 737
 Weller J., Albrecht A., 2002, Phys.Rev., D65, 103512
 Zlatev I., Wang L.-M., Steinhardt P. J., 1999, Phys. Rev. Lett., 82, 896

This paper has been typeset from a T_EX/ L^AT_EX file prepared by the author.